International Journal of Mass Spectrometry 459 (2021) 116469

Contents lists available at ScienceDirect

International Journal of Mass Spectrometry

journal homepage: www.elsevier.com/locate/ijms

To roam or not to roam, that is the question for the methyl group in isopropanol cations

Kyle J. Covert [a, 1], Andras Bodi [b], Krisztián G. Torma [a, 2], Krisztina Voronova [c], Tomas Baer [d], Bálint Sztáray [a, *]

[a] Department of Chemistry, University of the Pacific, Stockton, USA
[b] Laboratory for Synchrotron Radiation and Femtochemistry, Paul Scherrer Institute, Villigen, Switzerland
[c] Department of Chemistry, University of Nevada, Reno, Reno, USA
[d] Department of Chemistry, University of North Carolina, Chapel Hill, USA

ARTICLE INFO

Article history:
Received 15 October 2020
Received in revised form
29 October 2020
Accepted 1 November 2020
Available online 4 November 2020

ABSTRACT

Isopropanol (2-propanol) dissociatively photoionizes primarily into the CH_2CHOH^+, CH_3CHOH^+, $CH_3CHCH_3^+$ fragment ions, and, as a minor product, into $(CH_3)_2COH^+$ in the 10.0–13.1 eV photon energy range as shown by Imaging Photoelectron Photoion Coincidence (iPEPICO) spectroscopy. At internal energies of below 0.3 eV, the loss of CH_4 dominates *via* a roaming pathway, in which the leaving CH_3 abstracts a hydrogen atom from the other methyl group. At higher energies, the kinetically favored direct loss of a methyl radical quickly takes over as its transition state is looser. We use the measured CH_3-loss appearance energy of 10.44 ± 0.01 eV to confirm the heat of formation of protonated acetaldehyde, CH_3CHOH^+, as $\Delta_f H^\circ$ = 608 ± 1 kJ mol^{-1} at 0 K. The highest-energy dissociation observed leads to $CH_3CHCH_3^+$ + OH, which corresponds to C–O bond scission. This process is the premier example of a non-statistical dissociation which *can* be modeled using a statistical model, albeit with a physically meaningless appearance energy. This channel is shown to be non-statistical due to preferential OH loss from the first electronically excited ion state.

1. Introduction

2-Propanol, commonly known as isopropyl alcohol or simply IPA, is one of the most common household and industrial chemicals [1–3]. Short chain alcohols are also crucial components of fuel blends and their fragments contribute to radical chain propagation in low-temperature autooxidation [4–6]. What can possibly be learned from studying such a common, well-known molecule? It turns out that the 2-propanol cation is an ideal system to compare alkyl vs. alkane elimination kinetics and energetics. The competition between the two can be a complex and dynamic process. Alkyl elimination usually involves a simple bond cleavage while alkane elimination is typically a two-step process where the alkyl radical may undergo roaming to form a dipole-bound neutral–ion complex, followed by hydrogen transfer to the alkyl radical to form the closed-shell neutral leaving group [7]. Usually, the two processes compete at the same bond cleavage site. Whether the molecular ion loses a closed-shell alkane or open-shell alkyl radical depends on the dissociation kinetics as well as the energetic stability of the products, and one pathway may be preferred in only a narrow internal energy range [8–10]. Studying these competitive processes in 2-propanol presents an interesting challenge as, similar to acetone, it contains two, identical methyl groups, but, unlike acetone, there are three different sites with abstractable hydrogens, namely O–H, α-C–H, and β-C–H (see Table 1).

In the literature, both the methyl and methine groups have been implicated in the methane-dissociation mechanism [11–13]. Griffin et al. collected differential photoionization efficiency curves for 2-propanol and detected only methane elimination up to 100 meV above the ionization threshold at 10.1 eV [11]. However, methyl elimination quickly took over with as little as 100 meV more ion internal energy. Therefore, high-resolution internal energy selection of the molecular ion is required to study these dissociation processes.

While low-energy dissociation processes are difficult to study

* Corresponding author.
E-mail address: bsztaray@pacific.edu (B. Sztáray).
[1] present address: Agilent Technologies Inc., Santa Clara, USA.
[2] present address: BaySpec Inc., San Jose, USA.

https://doi.org/10.1016/j.ijms.2020.116469
1387-3806/

Table 1
Possible dissociation pathways of the 2-propanol molecular ion with the observed processes in bold.

Fragment Ion	Reaction Pathway		Thermochemical Limit (eV, G4)
m/z 59	→ **$(CH_3)_2COH^+ + H$**	**(1a)**	**10.24**
	→ $CH_2CH(OH)CH_3^+ + H$	(1 b)	10.91
	→ $(CH_3)_2CHO^+ + H$	(1c)	11.11
m/z 45	→ **$CH_3CHOH^+ + CH_3$**	**(2a)**	**10.43**
m/z 44	→ **$CH_2{=}CHOH^+ + CH_4$**	**(3a)**	**10.03**
	→ $CH_3CH{=}O^+ + CH_4$	(3 b)	10.49
	→ $CH_3C{=}OH^+ + CH_4$	(3c)	10.81
m/z 43	→ **$(CH_3)_2CH^+ + OH$**	**(4a)**	**11.53**

with electron ionization or even collision-induced dissociation, vacuum ultraviolet (VUV) photoionization is well-suited due to its high energy resolution [14]. Photoelectron photoion coincidence (PEPICO) detection with velocity map imaging for electrons allows for high-resolution parent ion internal energy selection while the use of a long ion acceleration region with moderate extraction fields can establish and quantify the dissociation kinetics in metastable processes [15,16]. Furthermore, the detailed photoionization mechanism may also help peak assignment in the study of complex reactive mixtures, in which imaging PEPICO has been shown to be a universal, sensitive, (isomer-)selective, and multiplexed detection tool [17]. As, according to the literature, 2-propanol has two competing unimolecular dissociation channels within a narrow energy range above its adiabatic ionization energy, the imaging PEPICO (iPEPICO) apparatus [18] at the VUV beamline [14] of the Swiss Light Source synchrotron in Villigen, Switzerland is ideally suited to study this system.

2. Experimental

The 2-propanol (anhydrous, 99.5%, from Sigma–Aldrich) sample was placed in a glass vial and the vapor was introduced from the headspace into the iPEPICO ionization region through an effusive inlet at room temperature. The pressure in the ionization chamber was set to $3–4 \times 10^{-6}$ mbar during measurements and the sample was ionized in a 2×2 mm^2 interaction region by the incident VUV synchrotron radiation in the photon energy region between 10.0 and 13.1 eV. Bending magnet radiation was collimated, dispersed by a 600 grooves/mm laminar grating and focused into a gas filter to remove higher harmonic radiation using a mixture of Ne, Ar, and Kr [19]. The photon energy was calibrated using the Ar 11s′–14s′ autoionization lines both in 1st and 2nd order. The photon energy resolution was measured to be better than 3 meV [18]. After photoelectrons and photoions were extracted in a constant 80 V cm^{-1} electric field, the electrons were velocity map imaged onto a Roentdek DLD40 position-sensitive delay-line detector, with a better than 1 meV electron kinetic energy resolution at threshold. Threshold electrons were focused to the center of the detector, together with kinetic energy ("hot") electrons with no off-axis momentum. A ring area around the center spot was chosen to represent and subtract the hot electron contamination from the center, yielding the threshold signal [20]. Photoions were mass analyzed by a two-stage Wiley–McLaren time-of-flight (TOF) mass spectrometer [18].

2.1. Statistical modeling

The breakdown diagram was modeled using rigid activated complex Rice–Ramsperger–Kassel–Marcus (rac-RRKM) theory [21,22]. The molecular ion's internal energy distribution and dissociation rate constants were calculated and the derived branching ratios were compared to the experimental breakdown diagram. The rac-RRKM unimolecular rate constants for each dissociation pathway, $k(E)$, were calculated as

$$k(E) = \frac{\sigma N^{\ddagger}(E - E_0)}{h\rho(E)}, \quad (1)$$

where σ is the symmetry number of the fragmentation channel, h is Planck's constant, $N^{\ddagger}(E - E_0)$ represents the number of states function for the transition state at internal energy $E - E_0$, and $\rho(E)$ is the density of states for the dissociating ion at internal energy E. The sums and densities of states were calculated using harmonic vibrational frequencies and the Beyer–Swinehart direct count algorithm [23].

2.2. Computational

The Gaussian 09 suite of programs were used to calculate, at the M06–2X/6–311++G (d,p) level of theory, the single-point energies and harmonic vibrational frequencies at the optimized geometries of the neutral molecule, the molecular ion, the various fragment ions and their corresponding neutral fragments involved in the unimolecular dissociation of 2-propanol [24,25]. The G4 composite method was then used to calculate more accurate energetics of the aforementioned stationary points [26]. W1U and CBS-QB3 methods were also employed to obtain a more accurate theoretical estimate for the adiabatic ionization energy of 2-propanol [27,28]. Tight transition states were located by relaxed potential energy scans along the bond length attributable to the reaction coordinates of interest and the saddle points thus identified were used as initial guess in transition state (TS) geometry optimizations. When gradually stretching the C–C bond, the methyl group was found, instead of leaving, to roam around the rest of the ion at less than 0.5 eV internal energy, forming an ion–neutral complex. As a well-defined TS could not be found by this potential energy scan alone, Born–Oppenheimer Molecular Dynamics (BOMD) simulations were employed to simulate this roaming dissociation channel, also to help visualize the movement of the CH_3 fragment after the C–C bond was broken [29]. The stopping criteria for these simulations was set to a leaving carbon–ion distance of 5 Å and allowed for the identification of the hydrogen atom abstracted from the ion to form the leaving methane neutral. These simulations suggested that the most likely pathway for internal H abstraction is from the other methyl group. A methyl-roaming transition state geometry could be identified, at which the roaming methyl group is approaching the opposing methyl group, prior to hydrogen abstraction. Vibrational frequency analysis confirmed the optimized structure to be a transition state with a low critical frequency, 176*i* cm^{-1}, closely corresponding to a carbon translational mode and implying a broad potential energy barrier along the reaction coordinate. The derived number of states function using the harmonic vibrational frequencies at this geometry was used as initial guess in the statistical model. Ultimately, the potential energy diagram (*vide infra*) was constructed using the G4 single point energies for all optimized structures [26]. Finally, we carried out time-dependent density functional theory (TDDFT) calculations using the B3LYP functional and the 6–311++G (d,p) basis set to help interpret the OH-loss mechanism.

2.3. Breakdown diagram

Threshold photoionization PEPICO TOF mass spectra of energy-selected 2-propanol cations were measured in the 10.0–13.1 eV

photon energy range. The area of each peak of interest was integrated in the hot-electron subtracted TOF spectra and then divided by the total intensity of all peaks to plot the breakdown diagram (fractional ion abundances vs. photon energy, Fig. 1) [20].

The abundance of the 2-propanol molecular ion (*m/z* 60) never amounts to 100% and starts out at ca. 80%. The reason for this is the shallow potential energy well of the 2-propanol molecular ion, into which the internal energy distribution of the neutral cannot fully transpose. The Franck–Condon factors are unfavorable for the origin transition, and the photoelectron spectrum (gray area in Fig. 1a) is structureless and the apparent onset of the photoelectron spectrum is not a reliable measure of the adiabatic ionization energy [30,31]. Therefore, a significant portion of 2-propanol is energetic enough to fragment into *m/z* 45 and 44 ions already at the ionization onset and the parent ion disappears from the breakdown diagram completely at already ca. 10.3 eV. These fragment ions correspond to a loss of a methyl radical and a methane molecule, respectively. According to our calculations (*vide infra*), the loss of a methane is the lowest-energy dissociation pathway and it is indeed the first major channel to appear in the experimental data, peaking at 10.3 eV with more than 60% abundance. Soon after the onset of the methane-loss *m/z* 44 ion, the methyl-loss *m/z* 45 also appears. It quickly becomes dominant in the breakdown diagram and stays so up to 13 eV photon energy, consistent with the photoionization mass spectrometry results of Griffin et al. [11] The competition between methane and methyl loss represents a classic case of kinetic control, where methane is both the more stable product and its dissociation is the lowest-energy pathway. However, as the leaving methyl group must pick up a hydrogen along the way to form methane, its transition state is tighter than that of simple methyl radical loss. Therefore, while the *m/z* 44 fragment ion dominates at low energies, its formation is quickly outcompeted by the energetically less favorable but entropically and kinetically favored simple methyl-loss dissociation.

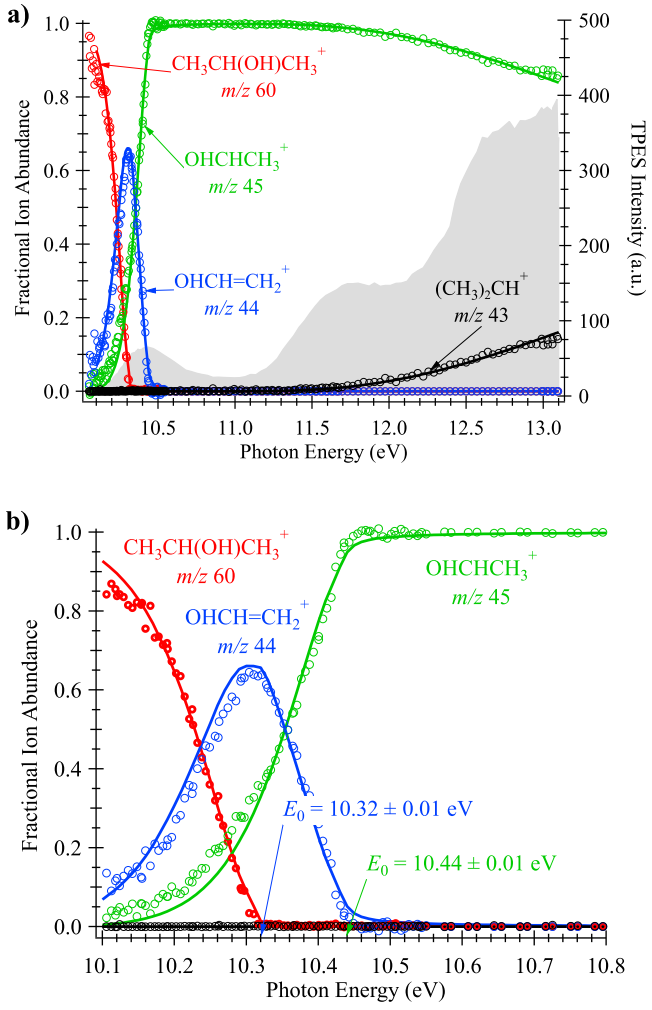

Fig. 1. a) Breakdown diagram of 2-propanol in the 10.0–13.1 eV photon energy range. The gray area shows the threshold photoelectron spectrum. b) The low-energy region of the breakdown diagram between 10.15 and 10.60 eV. Open circles represent experimental data points, and the solid lines show the statistical model.

We also observed hydrogen atom loss starting at about 10.5 eV, but it never amounted to more than 5% abundance. According to our calculations, the α-carbon is the most energetically favorable site to lose a hydrogen atom from, producing protonated acetone, $(CH_3)_2C{=}OH^+$. H loss is a minor dissociative photoionization (DPI) channel, and its 0 K appearance energy (E_0) could not be established with comparable uncertainty to even the most basic quantum-chemical computations. Therefore, it is omitted in the breakdown diagram in Fig. 1 and not included in the kinetic model. The highest-energy DPI channel in the studied energy range is the rise of *m/z* 43, which appears at around 11.5 eV and its fractional abundance rises quite slowly with increasing energy. This channel is most likely an OH radical loss from the molecular ion or, possibly, a consecutive H_2 loss from the methyl-loss CH_3CHOH^+ fragment ion. However, the slope of the breakdown curve is consistent with a dissociation that is in parallel with (and not consecutive to) methyl loss [22]. If the *m/z* 43 channel were consecutive loss of H_2 from *m/z* 45, its rise would be much more rapid, corresponding to the width of the energy distribution in the methyl-loss fragment ion. Considering it as an OH-loss dissociation indicates large competitive shift [31], due to the parallel and, at this energy, already quite fast methyl-loss dissociation channel that also originates from the 2-propanol molecular ion. However, as will be discussed later, this behavior it is most likely the result of non-statistical branching of the reactive flux in the energy range of the $\tilde{\mathbf{A}}^+$ cationic state.

The dissociative photoionization pathways of 2-propanol were explored by quantum chemical calculations for the plausible low-energy fragmentation pathways. A potential energy diagram containing these at the G4 level of theory is shown in Fig. 2.

***m/z* 45.** The direct methyl-loss pathway has no reverse barrier, and no saddle point was located when performing a relaxed potential energy scan along the C–C stretching coordinate. However, with respect to the internal rotation of the OH group, the two methyl groups are not equivalent and the one in *gauche* position with the hydroxyl is preferred to leave. Indeed, a relaxed potential energy scan along the C–C stretching coordinate of the methyl in *anti* configuration exhibits a small saddle point at 180 meV ion internal energy, corresponding to OH internal rotation in the CH_3CHOH^+ fragment ion. The calculated thermochemical limit of the methyl loss (2a) is 10.43 eV at the G4 level, which is in excellent agreement with the experimentally determined E_0 of 10.44 ± 0.01 eV.

***m/z* 44.** According to the experimental data, the lowest-energy channel is the loss of a methane molecule. As briefly discussed in the modeling section, there are three possible hydrogen-abstraction sites: the hydroxyl group, the α-, and β-carbons. If the dissociation is fast, there is no kinetic shift and the disappearance energy of the parent ion (at 10.32 eV in our case) corresponds to the 0 K appearance energy of the first fragment ion [22]. Therefore, it is quite clear from our calculations that the hydroxyl (3 b) and alpha carbon (3c) hydrogen-abstraction pathways are both too high in

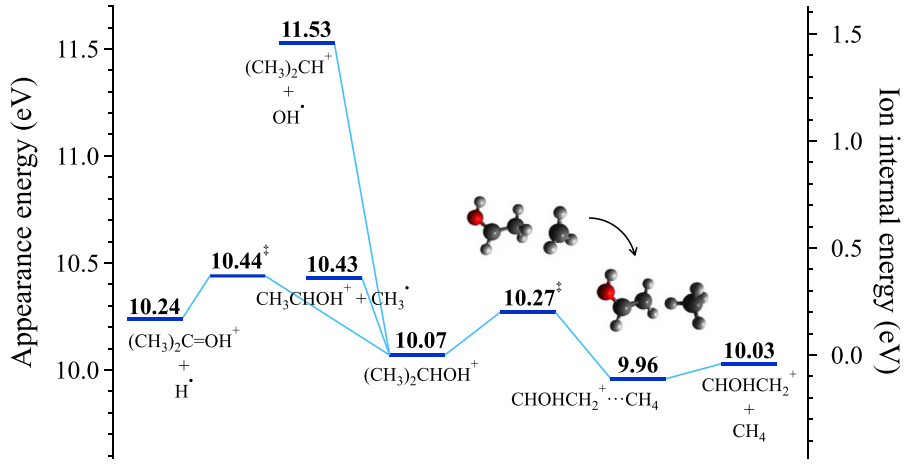

Fig. 2. Dissociation pathways of the 2-propanol cation. The zero-point corrected energies were calculated at the G4 level of theory relative to the neutral (left scale) and cationic 2-propanol (right scale).

energy, at 10.81 eV and 10.49 eV, respectively. Therefore, the abstracted hydrogen must come from the other beta carbon (3a) and the thermochemical limit leading to $CH_2{=}CHOH^+ + CH_4$ was found to be 9.95 eV at the G4 level. This thermochemical limit, however, does not correspond to the activation energy of the methane-loss channel and further calculations at various $^+CH_3CHOH\cdots CH_3$ distances helped elucidate the mechanism of the internal hydrogen abstraction. By increasing the distance between the departing methyl and the α-carbon in small steps and optimizing along the other internal coordinates, the methyl group does not leave outright, rather moves around the rest of the ion, in a shallow potential energy regime. Further stretching of the C—C bond then leads to dissociation along a purely attractive potential energy curve. However, from a position where the two methyl groups are in close propinquity, decreasing the C—C distance leads to a structure with a bridging hydrogen atom from the other methyl carbon. A local minimum features this hydrogen migrated over to the roaming methyl group, forming a loosely bound intermediate complex at 9.96 eV at the G4 level, on the way to the final CH_2CHOH^+ fragment ion and a methane neutral. A transition state search yielded a saddle point between this structure and the original molecular ion, with one imaginary vibrational frequency corresponding primarily to a methyl translation. The energy of this saddle point was calculated as 10.27 eV using G4 theory, which is in reasonable agreement with the experimentally determined E_0 of 10.32 ± 0.01 eV. Thus, the leaving methyl group can either undergo swift bond cleavage and product formation (at sufficient kinetic energy in the reaction coordinate), or it can orbit the cation center and roam over to opposite side by crossing this transition state region (at slightly lower energies). Once the methyl group is close enough for hydrogen abstraction, the formation of the leaving methane neutral takes place promptly and without a barrier. The competition between kinetically favored methyl loss and energetically favored methane loss invites a comparison with the DPI of acetone [10], where methane loss takes place exclusively by tunneling and can be shut down by perdeuteration. However, tunneling across an H-transfer barrier starts as a slow process at low energies, which should have shown up as an asymmetric daughter ion peak in the isopropanol PEPICO spectra. There is only little evidence of this happening as the methane-loss peak always appears to be symmetric and there is only a slight elevation of the baseline between the daughter and parent ion TOFs. This means that while there may be an H-transfer transition state, which is higher in energy than the methyl-roaming pathway, only trace amounts of methane loss may take place this way, through tunneling. The dominant roaming methane loss mechanism, however, is not affected by tunneling, as the relevant transition state corresponds to methyl transfer with a broad potential energy barrier. Then, once the internal energy is high enough to allow for direct methyl loss, methane loss is unable to compete with this fast process taking place through a loose transition state.

Thus, the dissociative photoionization mechanism can be separated into three energy regimes. At low energies, the parent ion is stable and only a small reactive flux may tunnel through an H-transfer transition state towards methane formation. At intermediate energies, the methyl group is still bound, but it may roam around the rest of the ion and eventually abstract a hydrogen atom to leave as neutral methane. This process is already fast at onset on the time scale of our experiment, yet it is much slower than direct methyl loss, which dominates as soon as it is energetically allowed. As mentioned above, this mechanism is in contrast with our earlier observations on the dissociative photoionization of the carbonyl-containing acetone [10], urea [32], and acetamide [33], where H-transfer preceded methane, isocyanic acid and ammonia formation. It is, however, similar to the roaming hydrogen-abstraction mechanism of the water-loss dissociation of energy-selected methyl hydroperoxide ions [34].

***m/z* 59.** Since the hydrogen-loss channel was only a minor pathway in the PEPICO experiments, amounting to less than 5% abundance, this channel was excluded from the statistical model. Quantum chemical calculations were nevertheless performed to elucidate the likely mechanism of this dissociation. While it is not possible to determine a reliable 0 K experimental appearance energy for this channel, it is already observed at 10.5 eV, which rules out an O—H bond cleavage (1c) or H loss from a methyl group (1 b) with G4 thermochemical limits of 11.11 eV and 10.91 eV, respectively. The alpha hydrogen loss (1a), however, has a calculated thermochemical limit of 10.24 eV, lower than the experimental onset of ca. 10.5 eV. A relaxed potential energy scan revealed a saddle point along the hydrogen-loss reaction coordinate, at 10.44 eV (G4 level), which is in line with the approximate experimental data.

***m/z* 43**. The highest-energy major fragmentation channel corresponds to a loss of the hydroxyl group and calculations at various DFT levels found a simple barrierless C—O bond scission. However, when we modeled this channel statistically (*vide infra*), the optimized E_0 of 11.01 eV was much lower than the G4-calculated thermochemical limit of 11.53 eV. This means that it is most

likely a modeling artifact as such an unphysically low value is needed to match the slope of this channel in the breakdown diagram. To understand the strange behavior of this channel, we turned to the DPI of methanol, where OH-loss takes place on the first electronically excited $\tilde{\mathbf{A}}^+ {}^2A\prime$ state surface [35]. However, in ethanol, slow hydrogen atom loss over a tight transition state is quickly outcompeted by methyl loss at higher energies and OH loss was not observed [30,36]. Hence, it is somewhat surprising to see OH loss reappear as a major channel in isopropanol.

In comparison with methanol's twelve internal degrees of freedom, isopropanol has thirty, which drastically increases the phase space of accessible nuclear geometries. Due to the OH-group orientation, the neutral C_1 minimum is chiral, but fast racemization occurs by tunneling through a C_S transition state at 0.037 eV (at G4 level). As far as the ground cation state is concerned, there are two isoenergetic and also chiral ionic minima. These stationary points can be expected to play a role in vertical ionizing transitions and this further complicates the dynamics of the dissociative photoionization process. Contrary to our findings for methanol, TD-DFT calculations suggest that the $\tilde{\mathbf{A}}^+$ state in the isopropanol cation, which lies in the energy range where the OH-loss fragmentation becomes abundant, is not isolated from the $\tilde{\mathbf{X}}^+$ state but the H–C–O–H torsional angle plays an important role in the coupling between these two states. Thus, these reaction coordinate scans do not explain the seemingly isolated state behavior of the $\tilde{\mathbf{A}}^+$ state satisfactorily and it is likely that excited state molecular dynamics calculations would be required to account for the non-statistical rise of the OH-loss signal. Since this is beyond the scope of this paper, our conclusion is based solely on experimental data that, in light of the unphysically low model appearance energy and the appearance of this fragment ion coinciding with the $\tilde{\mathbf{A}}^+$ state in the TPES, the OH-loss dissociation does not exhibit statistical behavior on the ground-state ion surface.

2.4. RRKM modeling of the breakdown diagram

The adiabatic ionization energy (AIE) of 2-propanol is evaluated to be 10.17 eV in the NIST Webbook and all of the referenced values there are above 10.0 eV [37]. Quantum chemical calculations at various levels of theory were performed to obtain reliable theoretical estimates for the AIE. Three different methods were used: G4, CBS-QB3, and W1U which gave 10.069 eV, 10.070 eV, and 10.078 eV, respectively, with an average AIE value of 10.072 eV. As we have previously reported, if the first dissociation onset (E_0) is close to the AIE and the potential energy well of the cation cannot support the internal energy distribution of the sample, the fractional abundance of the molecular ion may never reach 100%, because the high-energy tail of the internal energy distribution always reaches into the dissociative continuum [38]. Indeed, the significant noise below 10.1 eV is in line with the theoretical AIE of 10.072 eV.

The experimental ion abundances were modeled within the RRKM framework, as described earlier [22]. Ab initio vibrational frequencies and rotational constants were used to calculate the thermal energy distribution of the neutral precursor, and the densities and numbers of states in the rate equation. In the model, an ionization energy of 10.07 eV and a sample temperature of 298 K was used to calculate the parent molecule's thermal energy distribution. To fit the statistical model to the experimental breakdown curves, the appearance energies, E_0, of the three dissociation channels, as well as the transitional vibrational frequencies of the transition state models were optimized. The optimized breakdown diagram is shown in Fig. 1 along with the experimental data. The *m/z* 60 ion signal vanishes by 10.32 eV, thus the potential energy well of the molecular ion is at most only ≈0.25 eV deep. The model of the methane-loss channel included isomerization of the parent ion into an ion–neutral complex through an internal H-abstraction by the leaving methyl group. As discussed above, at low internal energies, < 0.3 eV, the leaving CH_3 group does not have enough energy to dissociate but forms a loosely bound $CH_4\cdots CH_2{=}CHOH^+$ complex. At higher than 0.3 eV of internal energy, however, the CH_3 group can dissociate directly through a loose transition state. The tightness of the roaming transition state leading to the $CH_4\cdots CH_2{=}CHOH^+$ complex is the deciding factor in the competition between the two pathways. Within a narrow energy range, the fractional abundance of the CH_4-loss channel drops to zero. The optimized methane loss E_0 corresponds to the barrier towards the ion–neutral complex formation and we obtained an appearance energy of 10.32 ± 0.01 eV, which is ca. 0.3 eV higher than the energy of the final products, while the E_0 for the methyl loss was found to be 10.44 ± 0.01 eV and corresponds to the thermochemical limit.

The highest-energy DPI channel of 2-propanol is the loss of a hydroxyl radical. To reproduce the branching ratios between the methyl and hydroxyl-loss channels, the statistical model optimized to an unrealistically low E_0 of 11.01 ± 0.02 eV with an activation entropy between that of methyl loss and the $H_3C\cdots H\cdots CH_2CHOH^+$ roaming transition state for methane loss. As mentioned earlier, the model's appearance energy is in clear disagreement with the literature E_0 of 11.501 ± 0.005 eV, calculated from heats of enthalpy of IPA, isopropylium ion, and hydroxyl radical, reported in the Active Thermochemical Tables (ATcT) [39]. The reason for this discrepancy, as discussed earlier, is that the OH-loss fragment ion formation kinetics cannot be described by a statistical rate model, because a more complex, non-statistical dissociative photoionization mechanism is at play. However, when non-statistical dissociation processes are in play, the breakdown curves cannot normally be reproduced even qualitatively by statistical rate theory [35,40–43] and the argument is routinely made that if statistical theory describes the breakdown curves adequately, the dissociation must be statistical [15]. Isopropanol is the first system in our practice, where this "duck test"[3] [44] of statisticality fails and only the correlation of the OH-loss breakdown curve with the photoelectron spectrum and, most importantly, the discrepancy between the calculated and modeled appearance energies reveal the non-statistical mechanism.

2.5. Thermochemistry

One of the two primary fragmentation channels, $(CH_3)_2CHOH \rightarrow CH_3CH{=}OH^+ + CH_3$, yielding protonated acetaldehyde, proceeds entirely along an attractive potential energy curve. Therefore, its appearance energy (E_0), which can be accurately determined from the breakdown diagram, corresponds to the thermochemical limit and it can be used to extract accurate thermochemical values. The heat of formation of the $CH_3CH{=}OH^+$ fragment ion can be obtained from its modeled appearance energy, E_0, and the well-established heats of formation of 2-propanol and the methyl radical:

$$\Delta_f H^o{}_{0K}[CH_3CH=OH^+] = \Delta_f H^o{}_{0K}[(CH_3)_2CHOH] - \Delta_f H^o{}_{0K}[CH_3] + E_0 \quad \text{add equation number, please (2)}$$

[3] If it looks like a duck, walks like a duck, and quacks like a duck, it must be a duck.

The E_0 obtained by fitting the RRKM model to the experimental breakdown curve is 10.44 ± 0.01 eV (1007 ± 1 kJ mol^{-1}). Using $\Delta_f H^o_{0K}$ [CH_3] = 149.872 ± 0.060 kJ mol^{-1} and $\Delta_f H^o_{0K}$ [$(CH_3)_2CHOH$] = −249.52 ± 0.38 kJ mol^{-1} from ATcT yields a gas-phase 0 K heat of formation of $\Delta_f H^o_{0K}$ [$CH_3CH{=}OH^+$] = 608 ± 1 kJ mol^{-1}, in excellent agreement with the latest ATcT value of 608.78 ± 0.40 kJ mol^{-1} [39]. This value is also consistent with and improves upon the computed 609.6 kJ mol^{-1} value we reported in a study of the dissociative photoionization of ethanol isotopologues [30].

3. Conclusion

The dissociative photoionization of 2-propanol was studied with imaging PEPICO spectroscopy, quantum chemical calculations and statistical modeling. Experimentally, 2-propanol has been found to dissociate primarily into CH_2CHOH^+, CH_3CHOH^+, $CH_3CHCH_3^+$, and, as a minor product, into $(CH_3)_2COH^+$ fragment ions in the photon energy range of 10.0–13.1 eV. The lowest-energy dissociation channel, yielding $CHOHCH_2^+ + CH_4$, is quickly outcompeted by the higher-energy, yet kinetically favored channel leading to $CH_3CHOH^+ + CH_3$, observed in the experimental breakdown curves and successfully modeled using an isomerization model. Both reactions are initiated by the CH_3 group moving away from the parent ion but, at internal energies below 0.3 eV, the loss of CH_4 dominates by way of a roaming pathway. That is, below the direct methyl-loss barrier, the CH_3 group cannot escape and may only orbit the fragment ion. Methane loss takes place when the roaming methyl group abstracts a hydrogen from the other methyl group. At higher internal energy, the direct loss of CH_3 dominates as the transition state leading to this fragmentation is much looser and, thus, kinetically favored. The competition between the alkyl and alkane elimination processes in the DPI of isopropanol is compared with that in acetone, urea and acetamide, in which direct H-transfer precedes alkane formation, as well as with methyl hydroperoxide, in which a roaming pathway has been reported. Quantum-chemical calculations also found a somewhat tight H-loss transition state lying slightly above the CH_3-loss threshold and leading to the minor, hydrogen-loss fragment ion $(CH_3)_2CH = OH^+$. The highest-energy dissociation observed in these experiments, leading to $CH_3CHCH_3^+ + OH$, is associated with simple C–O bond scission. This process can be modeled statistically, but only with an unphysically low barrier. This, together with TDDFT calculations and in comparison with the methanol and ethanol dissociative photoionization mechanisms suggest that OH loss is a non-statistical process, enhanced in the first electronically excited cation state. The statistical model fitted to the experimental data yielded accurate appearance energies corresponding to the thermochemical limit for the CH_3-loss dissociation as 10.44 ± 0.01 eV and the CH_4-loss as 10.32 ± 0.01 eV. By an ion cycle, the 0 K heat of formation of the CH_3CHOH^+ ion was found to be 608 ± 1 kJ mol^{-1}, in good agreement with both the ATcT value and a previous, computational result.

Credit Author Statement

Kyle J. Covert: Data acquisition, Formal analysis, Visualization, Writing - original draft. Andras Bodi: Formal analysis, Software, Conceptualization, Methodology, Writing - review & editing. Krisztián G. Torma: Data acquisition, Visualization, Formal analysis, Writing - review & editing. Krisztina Voronova: Data acquisition, Writing - review & editing. Tomas Bae: Conceptualization, Methodology, Writing - review & editing. Bálint Sztárayr: Data acquisition, Formal analysis, Software, Visualization, Writing - original draft, Writing - review & editing.

Declaration of competing interest

The authors declare that they have no known competing financial interests or personal relationships that could have appeared to influence the work reported in this paper.

Acknowledgments

This work has been funded by the National Science Foundation (Grant No. CHE-1665464) and by the Swiss Federal Office for Energy (BFE Contract No. SI/501269–01). We are grateful to Judit Zádor for her help with the roaming trajectory calculations.

References

[1] J. Klabunde, C. Bischoff, A.J. Papa, In Ullmann's Encyclopedia of Industrial Chemistry, Wiley-VCH Verlag GmbH & Co. KGaA, Weinheim, Germany, 2011, pp. 1–14.
[2] F.E.M. Alaoui, E.A. Montero, J.-P. Bazile, F. Aguilar, C. Boned, Liquid density of oxygenated additive 2-propanol at pressures up to 140MPa and from 293.15K to 403.15K, J. Chem. Thermodyn. 54 (2012) 358–365.
[3] J.R. Dunlop, F.P. Tully, Catalytic dehydration of alcohols by hydroxyl: 2-propanol; an intermediate case, J. Phys. Chem. 97 (1993) 6457–6464.
[4] A.M. Scheer, O. Welz, J. Zádor, D.L. Osborn, C.A. Taatjes, Low-temperature combustion chemistry of novel biofuels: resonance-stabilized QOOH in the oxidation of diethyl ketone, Phys. Chem. Chem. Phys. 16 (2014) 13027–13040.
[5] M. Almasi, M. Aynehband, Studies on thermodynamic properties of butyl acetate/alkan-2-ol binary mixtures: measurements and properties modeling, J. Mol. Liq. 225 (2017) 490–495.
[6] E.A. Montero, F. Aguilar, N. Muñoz-Rujas, F.E.M. Alaoui, Thermodynamic properties of propanol and butanol as oxygenate additives to biofuels, in: E. Jacob-Lopes, L.Q. Zepka (Eds.), Frontiers in Bioenergy and Biofuels, InTech, 2017.
[7] D.J. McAdoo, R.D. Bowen, Alkane eliminations from ions in the gas phase, Eur. J. Mass Spectrom. 5 (1999) 389–409.
[8] J.F. Litton, T.L. Kruger, R.G. Cooks, Alkane elimination in mass spectrometry. A counterpart to the McLafferty rearrangement, J. Am. Chem. Soc. 98 (1976) 2011–2013.
[9] J.L. Holmes, P.C. Burgers, Y.A. Mollah, Alkane elimination from ionized alkanols, org, Mass Spectrom. 17 (1982) 127–130.
[10] A. Bodi, T. Baer, N.K. Wells, D. Fakhoury, D. Klecyngier, J.P. Kercher, Controlling tunnelling in methane loss from acetone ions by deuteration, Phys. Chem. Chem. Phys. 17 (2015) 28505–28509.
[11] L.L. Griffin, J.C. Traeger, C.E. Hudson, D.J. McAdoo, Why are smaller fragments preferentially lost from radical cations at low energies and larger ones at high energies?: an experimental and theoretical study, Int. J. Mass Spectrom. 217 (2002) 23–44.
[12] J.-W. Shin, E.R. Bernstein, Experimental and theoretical studies of isolated neutral and ionic 2-propanol and their clusters, J. Chem. Phys. 130 (2009) 214306.
[13] J.R. Vacher, F. Jorand, N. Blin-Simiand, S. Pasquiers, Partial ionisation cross-sections of 2-propanol and ethanal, Chem. Phys. 323 (2006) 587–594.
[14] M. Johnson, A. Bodi, L. Schulz, T. Gerber, Vacuum ultraviolet beamline at the Swiss Light Source for chemical dynamics studies, Nucl. Instrum. Methods Phys. Res. 610 (2009) 597–603.
[15] T. Baer, B. Sztáray, J.P. Kercher, A.F. Lago, A. Bödi, C. Skull, D. Palathinkal, Threshold photoelectron photoion coincidence studies of parallel and sequential dissociation reactions, Phys. Chem. Chem. Phys. 7 (2005) 1507–1513.
[16] T. Baer, R.P. Tuckett, Advances in threshold photoelectron spectroscopy (TPES) and threshold photoelectron photoion coincidence (TPEPICO), Phys. Chem. Chem. Phys. 19 (2017) 9698–9723.
[17] A. Bodi, P. Hemberger, D.L. Osborn, B. Sztáray, Mass-resolved isomer-selective chemical analysis with imaging photoelectron photoion coincidence spectroscopy, J. Phys. Chem. Lett. 4 (2013) 2948–2952.
[18] A. Bodi, M. Johnson, T. Gerber, Z. Gengeliczki, B. Sztáray, Imaging photoelectron photoion coincidence spectroscopy with velocity focusing electron optics, Rev. Sci. Instrum. 80 (2009), 034101.
[19] P. Oßwald, P. Hemberger, T. Bierkandt, E. Akyildiz, M. Köhler, A. Bodi, T. Gerber, T. Kasper, In situ flame chemistry tracing by imaging photoelectron photoion coincidence spectroscopy, Rev. Sci. Instrum. 85 (2014), 025101.
[20] B. Sztáray, T. Baer, Suppression of hot electrons in threshold photoelectron photoion coincidence spectroscopy using velocity focusing optics, Rev. Sci. Instrum. 74 (2003) 3763–3768.
[21] T. Baer, W.L. Hase, Unimolecular Reaction Dynamics: Theory and Experiments, Oxford University Press, New York, 1996.
[22] B. Sztáray, A. Bodi, T. Baer, Modeling unimolecular reactions in photoelectron photoion coincidence experiments, J. Mass Spectrom. 45 (2010) 1233–1245.
[23] T. Beyer, D.F. Swinehart, Algorithm 448: number of multiply-restricted partitions, commun, ACM 16 (1973) 379.

[24] M.J. Frisch, G.W. Trucks, H.B. Schlegel, G.E. Scuseria, M.A. Robb, J.R. Cheeseman, G. Scalmani, V. Barone, B. Mennucci, G.A. Petersson, et al., Gaussian 09, Gaussian, Inc., Wallingford, CT, USA, 2009.
[25] Y. Zhao, D.G. Truhlar, The M06 suite of density functionals for main group thermochemistry, thermochemical kinetics, noncovalent interactions, excited states, and transition elements: two new functionals and systematic testing of four M06-class functionals and 12 other functionals, Theor. Chem. Account 120 (2008) 215–241.
[26] L.A. Curtiss, P.C. Redfern, K. Raghavachari, Gaussian-4 theory using reduced order perturbation theory, J. Chem. Phys. 127 (2007) 124105.
[27] G.D. Purvis, R.J. Bartlett, A full coupled-cluster singles and doubles model: the inclusion of disconnected triples, J. Chem. Phys. 76 (1982) 1910–1918.
[28] J.W. Ochterski, G.A. Petersson, J.A. Montgomery, A complete basis set model chemistry. V. Extensions to six or more heavy atoms, J. Chem. Phys. 104 (1996) 2598–2619.
[29] Gaussian 09 BOMD calculation, (accessed March 1, 2020).
[30] A. Bodi, M.D. Brannock, B. Sztáray, T. Baer, Tunneling in H Loss from energy selected ethanol ions, Phys. Chem. Chem. Phys. 14 (2012) 16047–16054.
[31] M.F. Heringa, J.G. Slowik, A.S.H. Prévôt, U. Baltensperger, P. Hemberger, A. Bodi, Dissociative ionization mechanism and appearance energies in adipic acid revealed by imaging photoelectron photoion coincidence, selective deuteration, and calculations, J. Phys. Chem. 120 (2016) 3397–3405.
[32] A. Bodi, P. Hemberger, T. Gerber, A robust link between the thermochemistry of urea and isocyanic acid by dissociative photoionization, J. Chem. Thermodyn. 58 (2013) 292–299.
[33] A. Bodi, P. Hemberger, Low-energy photoelectron spectrum and dissociative photoionization of the smallest amides: formamide and acetamide, J. Phys. Chem. 123 (2019) 272–283.
[34] K.J. Covert, K. Voronova, K.G. Torma, A. Bodi, J. Zádor, B. Sztáray, Thermochemistry of the smallest QOOH radical from the roaming fragmentation of energy selected methyl hydroperoxide ions, Phys. Chem. Chem. Phys. 20 (2018) 21085–21094.
[35] S. Borkar, B. Sztáray, A. Bodi, Dissociative photoionization mechanism of methanol isotopologues (CH_3OH, CD_3OH, CH_3OD and CD_3OD) by iPEPICO: energetics, statistical and non-statistical kinetics and isotope effects, Phys. Chem. Chem. Phys. 13 (2011) 13009–13020.
[36] A. Bodi, Internal energy selection in vacuum ultraviolet photoionization of ethanol and ethanol dimers, J. Chem. Phys. 139 (2013), 144306.
[37] Lias, S.G., Ion energetics data. In NIST Chemistry WebBook, NIST Standard Reference Database Number 69, P.J. Linstrom; W.G. Mallard, Eds., National Institute of Standards and Technology, Gaithersburg MD, 20899, (retrieved March 30, 2020).
[38] A. Bodi, Á. Kvaran, B. Sztáray, Thermochemistry of halomethanes CF_nBr_{4-n} (n = 0–3) based on iPEPICO experiments and quantum chemical computations, J. Phys. Chem. 115 (2011) 13443–13451.
[39] Ruscic, B.; Bross, D.H.Active Thermochemical Tables (ATcT) Values Based on Ver. 1.122g of the Thermochemical Network Available at ATcT.anl.Gov.
[40] R. Spezia, A. Martin-Somer, V. Macaluso, Z. Homayoon, S. Pratihar, W.L. Hase, Unimolecular dissociation of peptides: statistical vs. Non-statistical fragmentation mechanisms and time scales, Faraday Discuss 195 (2016) 599–618.
[41] K.-M. Weitzel, F. Güthe, J. Mähnert, R. Locht, H. Baumgärtel, Statistical and non-statistical reactions in energy selected fluoromethane ions, Chem. Phys. 201 (1995) 287–298.
[42] J. Harvey, A. Bodi, R.P. Tuckett, B. Sztáray, Dissociation dynamics of fluorinated ethene cations: from time bombs on a molecular level to double-regime dissociators, Phys. Chem. Chem. Phys. 14 (2012) 3935–3948.
[43] K. Voronova, K.G. Torma, J.P. Kercher, A. Bodi, B. Sztáray, Dissociative photoionization of chromium hexacarbonyl: a round-trip ticket to non-statisticality and a detective story in thermochemistry, Int. J. Mass Spectrom. 438 (2019) 63–71.
[44] M. Heim, Exploring Indiana Highways: Trip Trivia, 2007, p. 317.